Evaluating Cell Viability Heterogeneity Based on Information Fusion of Multiple Adhesion Strengths

Author list:

Mingji Wei, Rongbiao Zhang, Fei Zhang, Yecheng Zhang

Affiliation:

School of Electrical and Information Engineering, Jiangsu University, Zhenjiang, Jiangsu 212013, China

Correspondence

Rongbiao Zhang, School of Electrical and Information Engineering, Jiangsu University, Zhenjiang, Jiangsu 212013, China

E-mail address: zrb@ujs.edu.cn (R. Zhang)

ORCID

Mingji Wei http://orcid.org/0000-0002-6733-2670

Fei Zhang http://orcid.org/0000-0002-4445-3023

Abstract

Cell viability evaluation is significantly meaningful for cellular assays. Some cells with weak viability are easily killed in the detection of anti-cancer drugs, while others with strong viability survive and proliferate, ultimately leading to the treatment failure or the inaccuracy of biological assays. Accurately evaluating cell viability heterogeneity still remains difficult. This paper proposed a multi-physical property information fusion method for evaluating cell viability heterogeneity based on multiple linear regression (MLR) on a single-channel integrated microfluidic chip. In this method, adhesion strengths τ_N, that are defined as the magnitude of shear stress needed to detach (100-N) % of cell population, were extracted as the independent variables of MLR model by calculating the linear fitting of the impedance-response curves for shear stress (cell detachment assay). Besides, by calculating the non-linear fitting of the drug dose-response curves for cancer cells (IC_{50} assay), the half-maximal inhibitory concentration (IC_{50}) was extracted as the dependent variables of MLR model. The results show that the mean relative error of our fusion method reduces by 17.87% and 59.66% compared with the single-parameter method and the cell counting method. Moreover, through the theoretical analysis of the drug resistance heterogeneity model, it proved that there is a qualitative relationship between the cell adhesion strength and cell viability heterogeneity, which provides a theoretical basis for our fusion method.

KEYWORDS

Cell viability heterogeneity, Adhesion strengths, Multiple linear regression, Microfluidic chip, Shear stress

1 | INTRODUCTION

Cell viability heterogeneity defined as the difference in sensitivity of cell populations to anti-cancer drugs (Chisholm, Lorenzi, & Clairambault, 2016; Chou et al., 2017; Lavi, Greene, Levy, & Gottesman, 2013) is the leading reason for the inaccuracy of the anti-cancer drug clinical trials (Zhang, Xu, Yu, Shang, & Ye, 2018) and cell toxicology studies (Damiani, Solorio, Doyle, & Wallace, 2019). In the anti-cancer drug test, some cells with weak viability are easily killed, while others with strong viability survive and proliferate, resulting in treatment failure (Chou et al., 2017) or inaccurate dose-response analysis. Due to the difference in viability of individual cells, accurately evaluating the heterogeneity of cell population viability still remains difficult (Mao et al., 2018).

The traditional cell counting method evaluates cell viability by counting live cells in total cells (G. Li et al., 2018; R. Zhang et al., 2018), rather than distinguishing the heterogeneous cells in the live cell population. Since the electrochemical impedance spectroscopy (EIS) was first applied to the monitoring of cell dynamic events (Giaever & Keese, 1991), this method is widely accepted as a label-free, non-invasive, real-time and quantitative analytical approach for the assessment of cell viability (Wei, Zhang, Li, et al., 2019; Xu et al., 2016; R. Zhang et al., 2018). However, the sensitivity of measuring the impedance of a cell population with viability heterogeneity is too low to distinguish the difference of heterogeneous cells. Although tracking multiple properties of single cells using EIS method is feasible in some papers (Hong, Lan, & Jang, 2012; D. Ren & Chi, 2018; Tsai & Wang, 2016), the high-throughput detections of cell population heterogeneity still needs to be improved. In summary, those approaches talked above cannot distinguish heterogeneous cells in cell population. In addition, with the development of modern medicine, single-parameter evaluation of cell viability heterogeneity can no longer meet the requirements of the dose-response accuracy. The microfluidic technology (Chou et al., 2017; Liu, Zheng, & Jiang, 2019; Tavakoli et al., 2019) can achieve high-throughput measurements of cell multiple properties, such as membrane capacitance, cytoplasm conductivity and adhesion strength (X. Ren, Ghassemi, Babahosseini, Strobl, & Agah, 2017; Zhao et al., 2013; Zhao, Wang, Chen, Fan, & Huang, 2018; Y. Zheng, Shojaei-Baghini, Wang, & Sun, 2013; Zhou et al., 2018). It provides a technical basis for multi-parameter extraction of cell populations, but these parameters have not been used to

evaluate the heterogeneity of cell viability yet.

In this paper, a multiple linear regression method was used to predict the cell viability heterogeneity by fitting multiple parameters of adhesion strengths. Cell adhesion strength is a valuable biophysical marker of cell viability (Fuhrmann, Banisadr, Beri, Tlsty, & Engler, 2017; Gonzalez Garcia, Cantini, Ballesterbeltran, Altankov, & Salmeronsanchez, 2018; Peter et al., 2018). Here, adhesion strength τ_N is defined as the magnitude of shear stress needed to detach (100-N) % of cell population (Fuhrmann et al., 2017). As can be known from the integro-differential equation (IDE) nonlocal Lotka–Volterra model (Chisholm et al., 2016; Lavi et al., 2013), the overall expression of drug-resistant phenotype is closely related to the cell number with different drug-resistant degrees. In addition, the adhesion strength is qualitatively related to cell viability according to the cell detachment assay and IC_{50} assay. Therefore, the heterogeneity of cell viability can be expressed by corresponding adhesion strengths (Mao et al., 2018). For our approach, weakly adherent cells are washed away by smaller shear stress, while strongly adherent cells are detached by larger shear stress (Fuhrmann et al., 2017). Therefore, the extraction of multiple adhesion strengths in cell population can achieve the collection of cell drug-resistant gradient. Compared with the network-based prediction approaches that require large amounts of data, the multiple linear regression (MLR) is more appropriate in this paper.

Besides, a single-channel integrated microfluidic chip was designed for cell detachment assay to extract multiple parameters of adhesion strength. Microchannel was coated with fibronectin (FN) for specific adhesion, which has biological significance in studies *in vitro* (Fuhrmann et al., 2017; R. Li et al., 2017; Nguyen, Yin, Reyes, & Urban, 2013; Voiculescu et al., 2013). The EIS method (Chawla et al., 2018; Xu et al., 2016) was used to quantitatively measure the information of cell adhesion on the interdigitated electrode structures (IDES) array affected under different shear stresses. Although the impedance sensitivity is too low to distinguish the small changes in individual cell viability in a cell population, impedance can be used to monitor the changes of cell number in real time (Koo & Yun, 2016; R. Zhang et al., 2018). Because the normalized impedance is approximately linearly correlated with the number of cells attached to the electrodes (Wei, Zhang, Zhang, et al., 2019; Xiao, Lachance, Sunahara, & Luong, 2002). The results show that compared with the cell counting

method and the single-parameter method, our fusion method has significantly improved the accuracy of cell viability heterogeneity assessment.

2 | MATERIALS AND METHODS

2.1 | Cell culture and experimental setup

Human gastric cancer cells (SGC-7901 and BGC-823) are provided by Medical School, Jiangsu University (China). SGC-7901 and BGC-823 cells are cultured in Dulbecco's Modified Eagle's Medium (DMEM) supplemented with 10% fetal bovine serum (FBS) (Gibco, USA) at 37°C and 5% CO_2 inside a Water Jacketed CO_2 Incubator (Heal Force®). After cells are detached from cell culture dish using try-EDTA (Life Technologies GmbH, Darmstadt, Germany) for 2 min, cell culture medium is centrifuged at a speed of 600 rpm for 5 min. The supernatant solution is sucked away and replaced for 3 mL of new medium, and the cell culture medium containing about 10^6 cells/mL is mixed uniformly.

Impedance analyzer was purchased from Chenhua Instrument (Shanghai, China) and syringe pump was obtained from Baoding Shenchen Precision Pump Co., Ltd. (Hebei, China). Injectors with a volume of 5 mL were purchased from KLMEDICAL Apparatus Co., Ltd. (Zhenjiang, China). The microfluidic chip is fabricated by Wenhao Chip Technology Co., Ltd. (Suzhou, China) (see Figure 1a). The length, height and width of channel are 30 mm, 120 μm and 800 μm, respectively. Meanwhile, the diameter of channel port is 2 mm. A layer of the polydimethylsiloxane (PDMS) is bonded together with glass, which the gold IDES array is sputtered on. The microchannel was filled with 30 μg/mL of FN solution cultured for 2 h for special adhesion (Fuhrmann et al., 2017; Voiculescu et al., 2013). Then the FN solution was removed and the microfluidic chip was prepared for further assays. Moreover, the upper detection limit of this microfluidic chip is about 10^5 cells while the lower detection limit is about 100 cells.

2.2 | Cell detachment assay

In the cell detachment assay and IC_{50} assay (details see our previous work (Wei, Zhang, Zhang, et al., 2019)), the initial cell state and density were almost the same, for the cell culture medium was obtained from the same well mixed centrifuge tube. The cell medium was injected into the microfluidic chip and incubated for 8 h for adhesion. Adherent cells that

overgrow in the microchannel are considered as the control group. The normalized impedance (NI) is approximately proportional to the number of adhered cells. The NI is calculated according to the following equation:

$$\mathrm{NI}=\frac{Z_{cells}-Z_{cell-free}}{Z_{c}-Z_{cell-free}} \tag{1}$$

where Z_{cells} represents the impedance of cell adhesion in cell detachment assay, Z_c denotes the impedance of control group and $Z_{cell\text{-}free}$ denotes the impedance of no-cell adhesion.

After applying different magnitudes of shear stress (3-1000 dynes/cm^2) for 12 min, the cell detachment assay was performed by measuring the sensitive impedance at 1 kHz (see Figure 1b) (Fuhrmann et al., 2017). In fact, the response of NI to different shear stresses (exponential *x*-axis) is an *S*-shaped curve. For the convenience of calculations, some experimental data under lower shear stress or higher shear stress were removed before linear fitting by Origin2016. The fitting formula is as follows:

$$y = a\log x + b \tag{2}$$

where x represents the magnitude of shear stress, y represents the NI. Thus, the adhesion strengths τ_{25}, τ_{50}, τ_{75} can be calculated according to the formula:

$$x = 10^{\frac{y-b}{a}} \tag{3}$$

All experimental data are obviously statistically significant, i. e., $p<0.05$, where p means the differences between samples causing by sampling errors (Wei, Zhang, Li, et al., 2019).

2.3 | IC_{50} assay

Cell medium containing 10^6 cells/mL was dripped into 96-well plate (X2-X11), where X is from B to G. Each well of 96-well plate finally contains 100 μL of cell medium, which was incubated for 8 h for cell adhesion. Besides, the marginal wells of 96-well plate were filled with water in order to reduce the effect of sample group evaporation. A gradient of cell state was built by culturing cells with different concentrations of FBS for 24 h. Then, cisplatin (10 μL) of different concentrations (2-1000 μM) was dripped into each well of the sample groups cultured for 24 h (Böttger et al., 2019). 30 μL

of cell count kit-8 (CCK-8) was added to each well cultured for 0.5 h. Then the 96-well plate was put into Thermo Scientific Microplate Reader and was read at 450 nm wavelength. The cell index (CI) is calculated by the formula:

$$\mathrm{CI} = \frac{\mathrm{A}_s - \mathrm{A}_b}{\mathrm{A}_c - \mathrm{A}_b} \times 100\% \tag{4}$$

where A_s represents the absorbance of sample groups, A_c represents the absorbance control groups and A_b denotes the absorbance of water. Therefore, we obtained the response curve of cell index to different concentrations of anti-cancer drug, cisplatin. Also, the cell index response curve is a kind of *S*-shape curve. It is nonlinearly fitted by Origin2016 using Logistic function according to the formula:

$$y = \mathrm{A}_2 + \frac{\mathrm{A}_1 - \mathrm{A}_2}{1 + (\log x / x_0)^p} \tag{5}$$

where x represents the different concentrations of cisplatin and y denotes the cell index. IC_{50} can be calculated by the formula, which is given as:

$$x = 10^{\log_0\left(\left(\frac{\mathrm{A}_1 - \mathrm{A}_2}{y - \mathrm{A}_2} - 1\right)^{\frac{1}{p}}\right)} \tag{6}$$

All experimental data are obviously statistically significant, i. e., $p<0.05$, where p means the difference between samples causing by sampling errors (Wei, Zhang, Li, et al., 2019).

2.4 | Multiple linear regression

Multiple linear regression (MLR) creates an equation on the linear relationship between dependent and independent variables (X. Zheng et al., 2020). The MLR model can be expressed as:

$$y = b_0 + b_1 x_1 + \cdots + b_n x_n \tag{7}$$

where y is the dependent variable, x_1, x_2, …, x_n are independent variables. b_0 is the intercept and b_1 to b_n are the regression coefficients. In this paper, the function MATLAB Regress was used in analyzing the linear relationship between the logarithm of adhesion strengths and that of IC_{50}. The function MATLAB Regress is given as: [b, $b$int, r, $r$int] = regress (Y, X), where b denotes the regression coefficient, $b$int denotes the 95% confidence interval for the regression coefficient, r

denotes the residual, and *r*int denotes the 95% confidence interval for the residual. Usually, the performance of MLR model can be evaluated by the R-Square (COD), which is the coefficient of multiple determination (Wei, Zhang, Li, et al., 2019).

3 | Results and discussion

3.1 | Theoretical analysis on the model of drug resistance heterogeneity

An integro-differential equation (IDE) nonlocal Lotka–Volterra model with drug resistance phenotype structure is usually given as (Chisholm et al., 2016; Lavi et al., 2013):

$$\frac{\partial}{\partial t} n_C(\boldsymbol{m},t) = \left[\frac{r_C(\boldsymbol{m})}{1+k_C u_2(t)} - d_C(\boldsymbol{m}) I_C(t) - u_1(t)\mu_C(\boldsymbol{m}) \right] n_C(\boldsymbol{m},t) \tag{8}$$

where $n_C(m,t)$ is the expression of a drug resistance heterogeneity with the trait $\boldsymbol{m}$ and time t; the vector $m=[m_1, m_2, \ldots, m_n]$ denote the numbers of cancer cells with different sensitivities to drugs and the total cancer cells $M=\sum_{i=1}^{n} m_i$; t denotes the evolution time of the phenotypic trait in the population; r_C stands for the intrinsic proliferation rates of cancer cells; k_C denotes the influencing coefficient of the cytostatic drug; d_C is the death rates and μ_C is the drug sensitivity functions; I_C is the influencing term of environment that cell populations compete for space and nutrients; u_1 denotes the cytotoxic drug and u_2 denotes the cytostatic drug.

In this paper, the cytostatic drug was not used, i.e., $u_2=0$ and the IDE nonlocal Lotka–Volterra model is simplified as:

$$\frac{\partial}{\partial t} n_C(\boldsymbol{m},t) = \left[r_C(\boldsymbol{m}) - d_C(\boldsymbol{m}) I_C(t) - u_1(t)\mu_C(\boldsymbol{m}) \right] n_C(\boldsymbol{m},t) \tag{9}$$

and the whole expression of dose response is given as: $n_C=\sum_{i=1}^{n} n_C(m_i,t)$. The cell detachment assay and the IC_{50} assay revealed the potential relationship between the adhesion strength and the dose-response heterogeneity. So, define that the function $f(\cdot)$ represents the non-linear relationship between $\frac{m_i}{M}$ and $\frac{N_i - N_{i-1}}{100}$, where $\frac{m_i}{M}$ represents the percentage of cell

number with different sensitivities to drugs, $\frac{N_i - N_{i-1}}{100}$ represents the percentage of corresponding detached cells (see Figure 1c):

$$f\left(\frac{\boldsymbol{m}}{\mathrm{M}}\right) = \left[f\left(\frac{m_1}{\mathrm{M}}\right), f\left(\frac{m_2}{\mathrm{M}}\right), \ldots, f\left(\frac{m_n}{\mathrm{M}}\right)\right] = \left[\frac{N_1}{100}, \frac{N_2 - N_1}{100}, \ldots, \frac{N_n - N_{n-1}}{100}\right] \tag{10}$$

where $N_0 = 0, N_n = 100$ and τ_{100-N_i} denotes the magnitude of shear stress required to detach $N_i\%$ of cell population (Fuhrmann et al., 2017).

We know from formula (2) that:

$$\boldsymbol{N} = \boldsymbol{a} \log \tau_{100-N} + \boldsymbol{b} \tag{11}$$

where $N = [N_1, N_2, \ldots, N_n]$, $a = [a_1, a_2, \ldots, a_n]$ and $b = [b_1, b_2, \ldots, b_n]$ are the parameter vectors of linear fitting. Thus,

$$f\left(\frac{m_i}{\mathrm{M}}\right) = \frac{N_i - N_{i-1}}{100} = \frac{a_i \log \tau_{100-N_i} + b_i - a_{i-1} \log \tau_{100-N_{i-1}} - b_{i-1}}{100} \tag{12}$$

$$m_i = \mathrm{M} f^{-1}\left(\frac{a_i \log \tau_{100-N_i} + b_i - a_{i-1} \log \tau_{100-N_{i-1}} - b_{i-1}}{100}\right) \tag{13}$$

Combining formula (9) and (13), the cell adhesion strength is quantitatively related with the heterogeneity of cell viability. However, the drug sensitivity function μ_C is affected by different cell states and the types of drugs, thus calculating the drug resistance heterogeneity $n_C(m,t)$ by this model is quite difficult. So the relationship is commonly considered as qualitative and it provides the theoretical feasibility for evaluating cell viability heterogeneity using multiple adhesion strengths based on MLR model.

3.2 | Cell viability heterogeneity prediction using MLR

The adhesion strengths can be used to evaluate cell viability as was reported in our previous work (Wei, Zhang, Zhang, et al., 2019). Due to the lack of exact cell number gradients with different viabilities, the use of an adhesion strength parameter is not accurate. Therefore, the three parameters of adhesion strength τ_{25}, τ_{50} and τ_{75} were selected and fused

together through MLR model to predict the heterogeneity of cell viability. As is described in Figure 2a, the normalized impedance response to the logarithm of shear stress is linearly fitted for the convenience of calculations. The structure of MLR model is shown in Figure 2b.

Also, the cell index response to concentrations of cisplatin is a kind of *S*-shape curve, as can be seen in Figure 2c. The cell index response curves were nonlinearly fitted by Origin2016 using Logistic function. The IC_{50} was extracted according to formula (6). As can be seen in Figure 2b, the cell viability was considered as the dependent variable while the adhesion strengths were considered as the independent variables. Fitting 20 groups of data with MLR model can realize the prediction of IC_{50}.

In order to obtain more training models, cells were cultured with different concentrations of FBS to establish cell viability gradients. FBS provides cells with basic nutrition, growth and attachment factors (Pazoki et al., 2015). The Lack of FBS will lead to non-specific adhesion which has no biological significance in studies *in vitro*, thus the microchannel of the microfluidic chip was coated by FN for specific adhesion. Besides, non-specific adhesion can be ignored in this paper, because the adhesion strength of non-specific adherent cells is very weak and they are easily swept away by a lower flow rate. 10%, 2%, 0.5% and 0% FBS were chosen as the culturing conditions to establish the gradient of cell viability. It can be seen from Figure 3a that each r^2 of linear fitting as a multiple determination coefficient is greater than 0.82.

In addition, the r^2 of cell index response curves are all above 0.96 (see Figure 3b), this means quite perfect fitting.

TABLE 1 Data of multiple adhesion strengths and IC_{50}

samples	log[IC_{50}]	log[τ_{25}]	log[τ_{50}]	log[τ_{75}]
1	0.566	0.957	0.762	0.592
2	0.672	1.071	0.823	0.658
3	0.594	0.988	0.786	0.615
4	0.543	0.928	0.73	0.624
5	0.613	1.034	0.801	0.645
6	0.7	1.14	0.856	0.684

7	0.822	1.285	0.954	0.701
8	0.732	1.185	0.886	0.625
9	0.796	1.255	0.946	0.724
10	0.768	1.217	0.914	0.688
11	1.009	1.596	1.36	1.101
12	0.957	1.524	1.305	1.134
13	1.08	1.772	1.449	1.256
14	0.931	1.449	1.246	1.086
15	1.042	1.659	1.405	1.102
16	1.397	2.765	2.369	2.158
17	1.166	2.244	1.952	1.646
18	1.253	2.559	2.159	1.823
19	1.32	2.712	2.314	1.970
20	1.204	2.387	2.045	1.759

As can be seen from Table 1, 20 sample groups were obtained by repeating cell detachment assay and dose-response assay. The linear fitting result after rounding is given as:

$$y = 0.26 + 0.22x_1 + 0.28x_2 - 0.07x_3 \tag{14}$$

The confidence intervals for regression coefficients b_0, b_1, b_2, b_3 are [0.07, 0.45], [-0.54, 0.98], [-1.34, 1.90] and [-1.31, 1.18], respectively. The R^2 is 0.9447 in this MLR model, which means a quite excellent fitting. Meanwhile, the residuals of the MLR model in Figure 3c-d show that all residuals are below 0.1.

3.3 | Comparison among fusion method, single-parameter method and cell counting method

As was previously described in some papers (Fuhrmann et al., 2017), the single parameter of adhesion strength τ_{25} was calculated to represent the metastatic state of cancer cells. Here, we also calculated the mean relative error of single-

parameter method used for comparison among different evaluation methods. Firstly, 20 groups of τ_{25} and IC_{50} (SGC-7901 and BGC-823) were linearly fitted using Origin2016 (see Figure 4a and b), while 10 groups were tested calculating the mean relative error. Taking SGC-7901 cells as an example, this paper compared the accuracy of the single-parameter method and the fusion method. Cell counting assay was carried out along with the dose-response assay through manually counting cell number. The initial cell number in the dose-response assay was almost the same, but the IC_{50} was different due to the heterogeneity of cell viability.

The initial data of 20 groups were considered as the training groups, and another 10 groups were considered as the test groups. The relative errors of cell counting method, single-parameter method and fusion method were calculated by the formula (see Figure 4c):

$$E_{rk} = \frac{|N_k - N_k^*|}{N_k} \times 100\% \tag{15}$$

where E_{rk} denotes the relative error, $N = [N_1, N_2, \ldots, N_n], k \in [1, n]$ denotes the actual output and $N^{¿} = [N_1^{¿}, N_2^{¿}, \ldots, N_n^{¿}], k \in [1, n]$ denotes the ideal output.

The mean relative errors were calculated for comparison among different methods and they were obtained by the formula (see Figure 4d):

$$\overline{E} = \frac{\sum_{k=1}^{n} E_{rk}}{n} \tag{16}$$

As can be seen in Figure 4c, the relative errors of fusion method with 10% FBS are below 4.97%, while its mean relative error is 2.72%. The mean relative errors of the fusion method increase with the reduction of FBS concentrations. Because the denominator of the relative error formula decreases due to the FBS concentration reduction, causing the 8~fold differences of the relative errors. In fact, the absolute errors are almost the same.

Compared with single-parameter method and cell counting method, the mean relative error of fusion method averagely

reduces by 17.87% and 59.66%. It means that the fusion method can significantly improve the accuracy of cell viability heterogeneity evaluation. For multiple parameters, the adhesion strengths still belong to the single parameter in terms of biophysical properties. More parameters indicating cell state like membrane capacitance, cytoplasm conductivity and adhesion areas will be considered in the future.

4 | CONCLUSION

This paper proposed a multi-parameter fusion method based on MLR model to improve the accuracy of cell viability heterogeneity evaluation. The adhesion strengths τ_{25}, τ_{50} and τ_{75} were extracted by linearly fitting the response curve of normalized impedance to shear stress from cell detachment assay. In addition, the extraction of IC_{50} was obtained by nonlinearly fitting the response curve of drug to cisplatin from dose-response assay. 20 groups of the adhesion strengths and 20 corresponding groups of IC_{50} were used as the fitting groups of MLR model, and 10 groups were used as the test groups. The results show that, compared with the single-parameter method and the cell counting method, the mean relative error of fusion method is reduced by 17.87% and 59.66% on average. Besides, the theoretical analysis on the model of drug resistance heterogeneity proved that there is a quantitative/qualitative relationship between the cell adhesion strength and the cell viability heterogeneity, which provides a theoretical basis for fusion method to evaluate cell viability heterogeneity.

Three parameters of the adhesion strength still belong to the single parameter in the sense of cell biophysical characteristics. Many biophysical properties of cells like membrane capacitance, cytoplasm conductivity and adhesion areas are also related to the cell viability heterogeneity. Thus, more parameters will be considered in the future. Besides, the normalized impedance response to different shear stresses is actually a kind of *S*-shape curve. However, the response curves were linearly fitted for the convenience of calculations, and before that the experimental data measured under lower shear stresses and higher shear stresses were required to be manually removed. Manual operations are usually subjective and will cause the inaccuracy of parameter extraction, so the optimal fitting algorithm will be developed in the future.

ACKNOWLEDGMENTS

This work was financially supported by the National Natural Science Foundation of China (grant no. 61673195), the N atural Science Research of Jiangsu Higher Education Institutions of China (CN) (grant no. 18KJB510008), a Project Funded

by the Priority Academic Program Development of Jiangsu Higher Education Institutions (no. PAPD-2018-87) and the Postgraduate Research & Practice Innovation Program of Jiangsu Province [grant no. KYCX20_3029].

DECLARATION OF COMPETING INTEREST

The authors declare no competing financial interest.

FIGURE

Figure 1

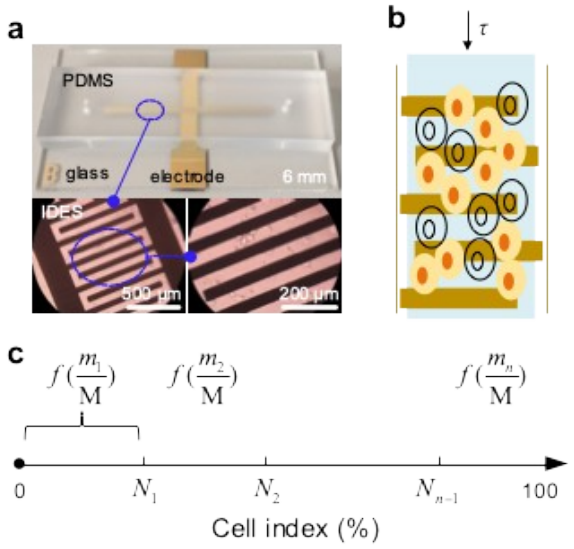

Figure 2

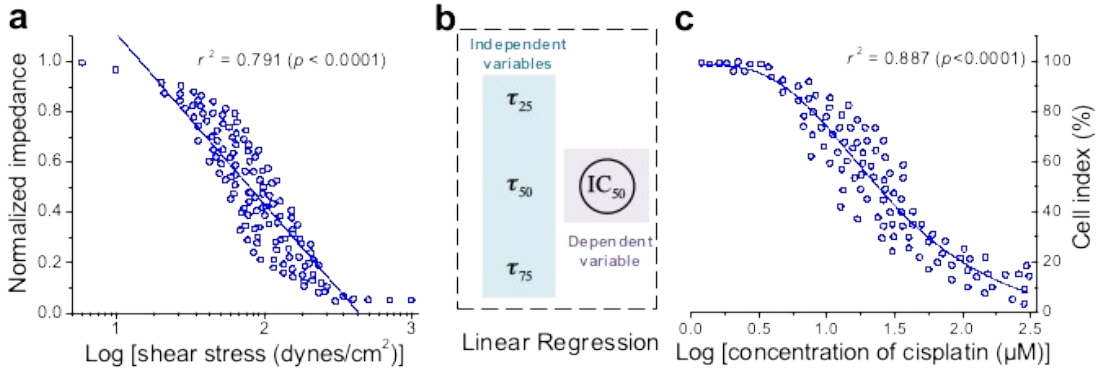

Figure 3

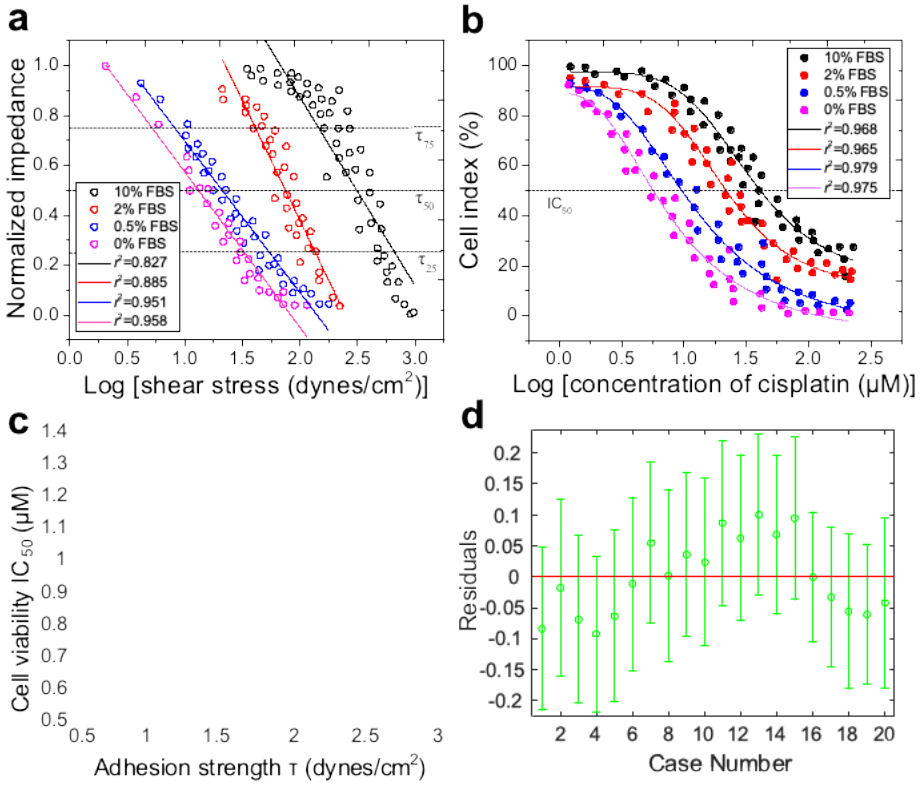
a
Normalized impedance
Log [shear stress (dynes/cm²)]
10% FBS
2% FBS
0.5% FBS
0% FBS
r²=0.827
r²=0.885
r²=0.951
r²=0.958
τ75
τ50
τ25
b
Cell index (%)
Log [concentration of cisplatin (μM)]
IC50
r²=0.968
r²=0.965
r²=0.979
r²=0.975
c
Cell viability IC50 (μM)
Adhesion strength τ (dynes/cm²)
d
Residuals
Case Number

Figure 4

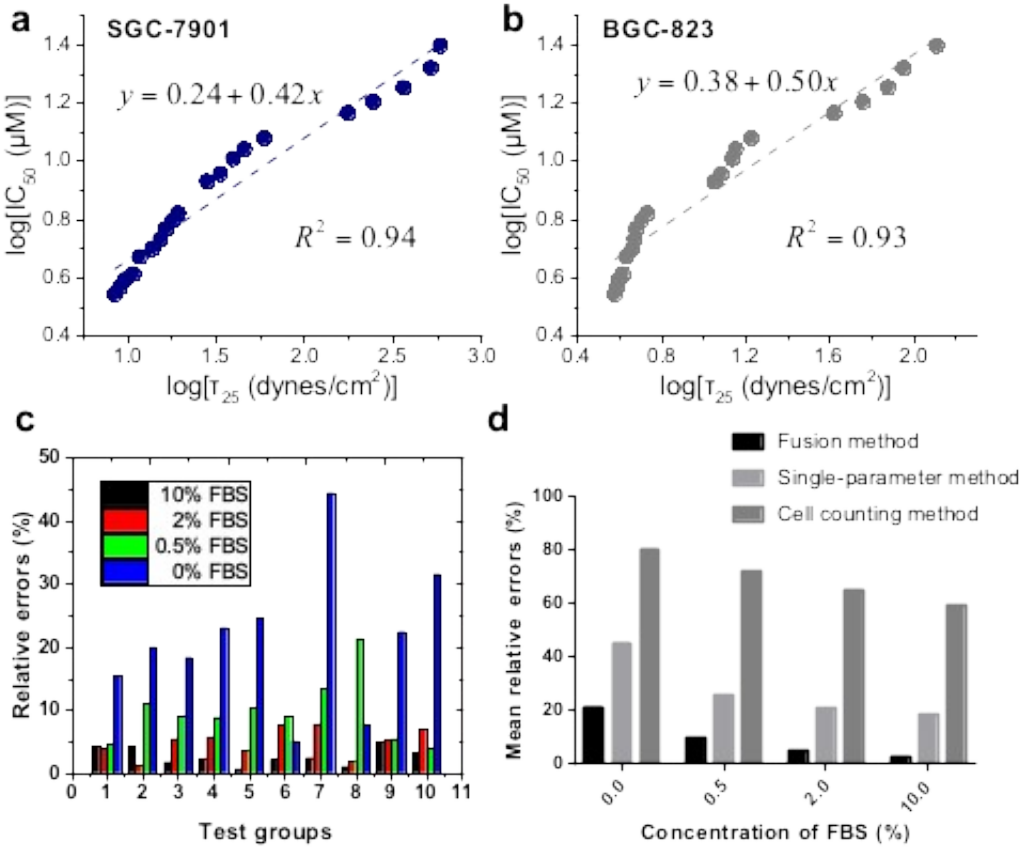
a
SGC-7901
y = 0.24 + 0.42x
R² = 0.94
log[IC50 (μM)]
log[τ25 (dynes/cm²)]
b
BGC-823
y = 0.38 + 0.50x
R² = 0.93
c
Relative errors (%)
Test groups
10% FBS
2% FBS
0.5% FBS
0% FBS
d
Fusion method
Single-parameter method
Cell counting method
Mean relative errors (%)
Concentration of FBS (%)

REFERENCES

Böttger, F., Semenova, E. A., Song, J.-Y., Ferone, G., van der Vliet, J., Cozijnsen, M., . . . Berns, A. (2019). Tumor Heterogeneity Underlies Differential Cisplatin Sensitivity in Mouse Models of Small-Cell Lung Cancer. *Cell Reports, 27*(11), 3345-3358. doi:https://doi.org/10.1016/j.celrep.2019.05.057

Chawla, K., Modena, M. M., Ravaynia, P. S., Lombardo, F. C., Leonhardt, M., Panic, G., . . . Hierlemann, A. (2018). Impedance-Based Microfluidic Assay for Automated Antischistosomal Drug Screening. *ACS Sensors, 3*(12), 2613-2620. doi:https://doi.org/10.1021/acssensors.8b01027

Chisholm, R. H., Lorenzi, T., & Clairambault, J. (2016). Cell population heterogeneity and evolution towards drug resistance in cancer: Biological and mathematical assessment, theoretical treatment optimisation. *Biochimica et Biophysica Acta (BBA) - General Subjects, 1860*(11), 2627-2645. doi:https://doi.org/10.1016/j.bbagen.2016.06.009

Chou, W.-P., Wang, H.-M., Chang, J.-H., Chiu, T.-K., Hsieh, C.-H., Liao, C.-J., & Wu, M.-H. (2017). The utilization of optically-induced-dielectrophoresis (ODEP)-based virtual cell filters in a microfluidic system for continuous isolation and purification of circulating tumour cells (CTCs) based on their size characteristics. *Sensors and Actuators B: Chemical, 241*, 245-254. doi:https://doi.org/10.1016/j.snb.2016.10.075

Damiani, E., Solorio, J. A., Doyle, A. P., & Wallace, H. M. (2019). How reliable are in vitro IC 50 values? Values vary with cytotoxicity assays in human glioblastoma cells. *Toxicology Letters, 302*, 28-34. doi:https://doi.org/10.1016/j.toxlet.2018.12.004

Fuhrmann, A., Banisadr, A., Beri, P., Tlsty, T. D., & Engler, A. J. (2017). Metastatic State of Cancer Cells May Be Indicated by Adhesion Strength. *Biophysical Journal, 112*(4), 736-745. doi:https://doi.org/10.1016/j.bpj.2016.12.038

Giaever, I., & Keese, C. R. (1991). Micromotion of mammalian cells measured electrically. *Proceedings of the National Academy of Sciences of the United States of America, 88*(17), 7896-7900. doi:https://doi.org/10.1073/pnas.90.4.1634-b

Gonzalez Garcia, C., Cantini, M., Ballesterbeltran, J., Altankov, G., & Salmeronsanchez, M. (2018). The strength of the protein-material interaction determines cell fate. *Acta Biomaterialia, 77*, 74-84. doi:https://doi.org/10.1016/j.actbio.2018.07.016

Hong, J. L., Lan, K.-C., & Jang, L.-S. (2012). Electrical characteristics analysis of various cancer cells using a microfluidic device based on single-cell impedance measurement. *Sensors & Actuators B Chemical, 173*, 927-934. doi:https://doi.org/10.1016/j.snb.2012.06.046

Koo, Y., & Yun, Y. (2016). Effects of polydeoxyribonucleotides (PDRN) on wound healing: Electric cell-substrate impedance sensing (ECIS). *Mater Sci Eng C Mater Biol Appl, 69*, 554-560. doi:https://doi.org/10.1016/j.msec.2016.06.094

Lavi, O., Greene, J. M., Levy, D., & Gottesman, M. M. (2013). The Role of Cell Density and Intratumoral Heterogeneity in Multidrug Resistance. *Cancer Research, 73*(24), 7168-7175. doi:https://doi.org/10.1158/0008-5472.can-13-1768

Li, G., Zhang, R., Yang, N., Yin, C., Wei, M., Zhang, Y., & Sun, J. (2018). An approach for cell viability online detection based on the characteristics of lensfree cell diffraction fingerprint. *Biosensors & Bioelectronics, 107*, 163. doi:https://doi.org/10.1016/j.bios.2018.01.047

Li, R., Zhang, X., Lv, X., Geng, L., Li, Y., Qin, K., & Deng, Y. (2017). Microvalve controlled multi-functional microfluidic chip for divisional cell co-culture. *Analytical Biochemistry, 539*, 48-53. doi:https://doi.org/10.1016/j.ab.2017.10.008

Liu, X., Zheng, W., & Jiang, X. (2019). Cell-Based Assays on Microfluidics for Drug Screening. *ACS Sensors, 4*(6), 1465-1475. doi:https://doi.org/10.1021/acssensors.9b00479

Mao, S., Zhang, W., Huang, Q., Khan, M., Li, H., Uchiyama, K., & Lin, J. M. (2018). InSitu Scatheless Cell Detachment Reveals Correlation between Adhesion Strength and Viability at Single−Cell Resolution. *Angewandte Chemie International Edition*. doi:https://doi.org/10.1002/anie.201710273

Nguyen, T. A., Yin, T.-I., Reyes, D., & Urban, G. A. (2013). Microfluidic Chip with Integrated Electrical Cell-Impedance Sensing for Monitoring Single Cancer Cell Migration in Three-Dimensional Matrixes. *Analytical Chemistry, 85*(22), 11068-11076. doi:https://doi.org/10.1021/ac402761s

Pazoki, H., Eimani, H., Farokhi, F., Shahverdi, A., Salman Yazdi, R., & Tahaei, L. (2015). Comparing the growth and the development of mouse pre-antral follicle in medium with PL (Platelet Layset) and with FBS. *Middle East Fertility Society Journal, 9*(4), 231-236. doi:https://doi.org/10.1016/j.mefs.2015.01.006

Peter, B., Ungai-Salanki, R., Szabo, B. i., ‡, Nagy, A. G., Szekacs, I., . . . Robert. (2018). High-Resolution Adhesion Kinetics of EGCG-Exposed Tumor Cells on Biomimetic Interfaces: Comparative Monitoring of Cell Viability Using Label-Free Biosensor and Classic End-Point Assays. *Acs Omega, 3*(4), 3882-3891. doi:https://doi.org/10.1021/acsomega.7b01902

Ren, D., & Chi, O. C. (2018). Feasibility of Tracking Multiple Single-Cell Properties with Impedance Spectroscopy. *ACS Sensors, 3*, 1005-1015. doi:https://doi.org/10.1021/acssensors.8b00152

Ren, X., Ghassemi, P., Babahosseini, H., Strobl, J. S., & Agah, M. (2017). Single-Cell Mechanical Characteristics Analyzed by Multiconstriction Microfluidic Channels. *ACS Sensors, 2*(2), 290-299. doi:https://doi.org/10.1021/acssensors.6b00823

Tavakoli, H., Zhou, W., Ma, L., Perez, S., Ibarra, A., Xu, F., . . . Li, X. (2019). Recent advances in microfluidic platforms for single-cell analysis in cancer biology, diagnosis and therapy. *TrAC Trends in Analytical Chemistry, 117*, 13-26. doi:https://doi.org/10.1016/j.trac.2019.05.010

Tsai, S. L., & Wang, M.-H. (2016). 24 h observation of a single HeLa cell by impedance measurement and numerical modeling. *Sensors & Actuators B Chemical, 229*, 225-231. doi:https://doi.org/10.1016/j.snb.2016.01.107

Voiculescu, I., Li, F., Liu, F., Zhang, X., Cancel, L. M., Tarbell, J. M., & Khademhosseini, A. (2013). Study of long-term viability of endothelial cells for lab-on-a-chip devices. *Sensors & Actuators B Chemical, 182*, 696-705. doi:https://doi.org/10.1016/j.snb.2013.03.030

Wei, M., Zhang, R., Zhang, F., Zhang, Y., Li, G., Miao, R., & Shao, S. (2019). An Evaluation Approach of Cell Viability Based on Cell Detachment Assay in a Single-Channel Integrated Microfluidic Chip. *ACS Sensors, 4*(10), 2654-2661. doi:https://doi.org/10.1021/acssensors.9b01061

Wei, M., Zhang, Y., Li, G., Ni, Y., Wang, S., Zhang, F., . . . Wang, P. (2019). A cell viability assessment approach based on electrical wound-healing impedance characteristics. *Biosensors and Bioelectronics, 124-125*, 25-32. doi:https://doi.org/10.1016/j.bios.2018.09.080

Xiao, C., Lachance, B., Sunahara, G., & Luong, J. H. T. (2002). An in-depth analysis of electric cell-substrate impedance sensing to study the attachment and spreading of mammalian cells. *Analytical Chemistry, 74*(6), 1333-1339. doi:https://doi.org/10.1021/ac011104a

Xu, Y., Xie, X., Duan, Y., Wang, L., Cheng, Z., & Cheng, J. (2016). A review of impedance measurements of whole cells. *Biosensors and Bioelectronics, 77*, 824-836. doi:https://doi.org/10.1016/j.bios.2015.10.027

Zhang, R., Wei, M., Chen, S., Li, G., Zhang, F., Yang, N., & Huang, L. (2018). A cell viability assessment method based on area-normalized impedance spectrum (ANIS). *Biosensors & Bioelectronics, 110*, 193-200. doi:https://doi.org/10.1016/j.bios.2018.03.041

Zhang, Y., Xu, J., Yu, Y., Shang, W., & Ye, A. (2018). Anti-Cancer Drug Sensitivity Assay with Quantitative Heterogeneity Testing Using Single-Cell Raman Spectroscopy. *Molecules, 23*(11). doi:https://doi.org/10.3390/molecules23112903

Zhao, Y., Chen, D., Li, H., Luo, Y., Deng, B., Huang, S.-B., . . . Chen, J. (2013). A microfluidic system enabling continuous characterization of specific membrane capacitance and cytoplasm conductivity of single cells in suspension. *Biosensors and Bioelectronics, 43*, 304-307. doi:https://doi.org/10.1016/j.bios.2012.12.035

Zhao, Y., Wang, K., Chen, D., Fan, B., & Huang, C. (2018). Development of microfluidic impedance cytometry enabling the quantification of specific membrane capacitance and cytoplasm conductivity from 100,000 single cells. *Biosensors & Bioelectronics, 111*, 138-143. doi:https://doi.org/10.1016/j.bios.2018.04.015

Zheng, X., Jiang, Z., Ying, Z., Song, J., Chen, W., & Wang, B. (2020). Role of feedstock properties and hydrothermal carbonization conditions on fuel properties of sewage sludge-derived hydrochar using multiple linear regression technique. *Fuel, 271*, 117609. doi:https://doi.org/10.1016/j.fuel.2020.117609

Zheng, Y., Shojaei-Baghini, E., Wang, C., & Sun, Y. (2013). Microfluidic characterization of specific membrane capacitance and cytoplasm conductivity of single cells. *Biosensors & Bioelectronics, 42*, 496-502. doi:https://doi.org/10.1016/j.bios.2012.10.081

Zhou, Y., Yang, D., Zhou, Y., Khoo, B. L., Han, J., & Ai, Y. (2018). Characterizing Deformability and Electrical Impedance of Cancer Cells in a Microfluidic Device. *Analytical Chemistry, 90*, 912-919. doi:https://doi.org/10.1021/acs.analchem.7b03859

FIGURE LEGENDS

FIGURE 1 Experimental setup and schematic diagram. (a) An integrated microfluidic chip with cells adherent on IDES. The scale bar is shown in continuously enlarged graphs. (b) A diagram of the cells partially detaching from IDES under the exposure to flow shear stress τ. (c) The explanation diagram on the mathematical definition of the number of cancer cells with different sensitivities to drug, $\boldsymbol{m}$.

FIGURE 2 Extraction of adhesion strength parameters for cell viability evaluation based on MLR. (a) Linear fitting of normalized impedance response to flow shear stress. (b) The structure of linear regression. The adhesion strengths τ_{25}, τ_{50}, τ_{75} are the independent variables and IC_{50} is the dependent variable of MLR model. (c) Cell index response to different concentrations of cisplatin.

FIGURE 3 Parameters extraction and prediction of IC_{50}. (a) Linear fitting of normalized impedance response to flow shear stress with different concentrations of FBS. Adhesion strength τ_{25}, τ_{50}, τ_{75} are extracted. (b) Nonlinear fitting of cell index response to different concentrations of cisplatin with different concentrations of FBS. IC_{50} is extracted. (c) The results of linear regression. '+' represents actual values and the red line represents the prediction values. (d) The residual case order plot of MLR model.

FIGURE 4 Single-parameter linear regression of SGC-7901 (a) and BGC-823 (b) cells. The relative errors of test groups using the fusion method. (b) Comparison of mean relative errors among the fusion method, single-parameter method and cell counting method.